Thermal Modal Analysis of Doubly Curved Shell Based on Rayleigh-Ritz Method

*ZHANG Yongfeng, ZHU Ziyuan, WANG Gang**

School of Mechanical and Electric Engineering, Soochow University, Suzhou 215131, P. R. China

(Received 6 January 2022; revised 16 January 2022; accepted 23 February 2022)

Abstract: The doubly curved shell (DCS) is a common structure in the engineering field. In a thermal environment, the vibration characteristics of the DCS will be affected by the thermal effect. The research on the vibration characteristics of DCS in thermal environment is relatively limited. In this paper, the thermal strain and the change of Young's modulus caused by the changing of temperature are studied, and the DCS energy equation is established systematically. The displacement tolerance function of the DCS is constructed by the spectral geometry method, and the natural frequencies and mode shapes of the DCS with different structural parameters, such as thicknesses, ratios of R_a/R_b and a/b, at different temperatures are solved by the Rayleigh-Ritz method. The results show that the natural frequency of the DCS decreases with the increasing temperature, R_a/R_b and a/b ratios, and increases with the increasing thickness.

Key words: doubly curved shell; thermal environment; Rayleigh-Ritz method; natural frequencies

CLC number: TB31 **Document code:** A **Article ID:** 1005-1120(2022)01-0058-08

0 Introduction

The doubly curved shell is widely used in aerospace, marine engineering, vehicle engineering, civil construction, machinery and other related engineering fields. Therefore, it is necessary to study the vibration characteristics of the doubly curved shell (DCS) in thermal environments. Huu et al.[1] analyzed the free vibration of simply supported the doubly curved shell on elastic foundations in thermal environments and deduced the motion control equation based on first-order shear deformation theory and the Hamiltonian principle. Alijani et al.[2-3] investigated nonlinear forced vibrations of functionally graded material (FGM) doubly curved shallow shells with rectangular and thermal effects. Yazdi[4] investigated the large amplitude vibration of moderately thick three-phase multiscale composite doubly curved shells. Viola et al.[5] provided a general framework for the formulation and dynamic analysis computations of moderately thick laminated doubly-curved shells and shells. Sofiyev et al.[6] analyzed the large amplitude vibration behavior of functionally graded orthotropic double-curved shallow shells, and various examples revealed that the influence of heterogeneity was noticeable. Ghorbanpour[7] studied the critical temperature rise of cylindrical shells based on higher-order stability equations. Li et al.[8] analyzed the free vibration of cylindrical shells with temperature-dependent material properties. Tornabene et al.[5] studied the differences between the well-known first-order shear deformation theory (FSDT) and several higher-order shear deformation theories (HSDTs) and established[9] the displacement field formulation of laminated composite shell structures with variable radii of curvature by HSDTs. Dastjerdi et al.[10-11] studied the non-linear dynamic analysis of torus-shaped and cylindrical shell-like structures and presented[12] a single general formulation for the analysis of various shell-shaped structures, including cylindrical, conical, spherical, elliptical, hyperbolic, parabolic. Karimi-

*Corresponding author, E-mail address: wanggang81@suda.edu.cn.

How to cite this article: ZHANG Yongfeng, ZHU Ziyuan, WANG Gang. Thermal modal analysis of doubly curved shell based on Rayleigh-Ritz method[J]. Transactions of Nanjing University of Aeronautics and Astronautics, 2022, 39(1): 58-65.

http://dx.doi.org/10.16356/j.1005-1120.2022.01.006

asl et al.[13] investigated the post-buckling behaviors of doubly curved composite shells in hygro-thermal environment by employing multiple scales perturbation method.

Based on the Rayleigh-Ritz method, four sets of springs with adjustable stiffness are introduced at the boundary of the DCS to simulate various boundary conditions in this paper. The displacement tolerance function based on the spectral geometry method is used to ensure the continuity of the boundary of the shell, and the vibration characteristics of doubly curved shells are calculated by considering the thermal strain.

1 Theoretical Analysis

The geometry and coordinate system of the doubly curved shell are shown in Fig. 1. Four groups of virtual springs are introduced around the doubly curved shell to simulate the boundary conditions.

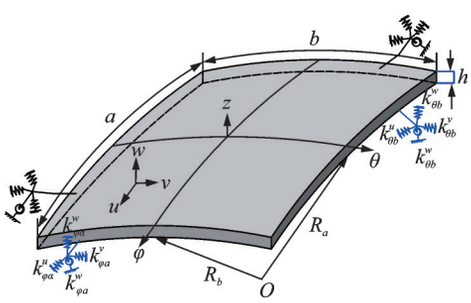

Fig.1 Geometry and coordinate system of doubly curved shell

In Fig.1, φ, θ and z represent the two circumferential and normal coordinates of the doubly curved shell, respectively; and u, v and w represent the displacements of the middle surface of the shell in the directions φ, θ and z, respectively; a and b represent the arc lengths of the shell in the directions φ and θ, respectively; R_a and R_b represent the curvature radius of the shell in the directions φ and θ, respectively; h is the shell thickness in the direction of the z-axis direction. In Fig.1, three sets of linear displacement constraint springs ($k^u_{\varphi a}$, $k^v_{\varphi a}$, $k^w_{\varphi a}$) and one set of rotary constraint springs ($K^w_{\varphi a}$) are set along the three coordinates φ, θ, and z directions located at $\varphi=a$, respectively (stiffness constants for other springs are defined similarly).

The Rayleigh-Ritz method is employed to solve the free vibration problem of the DCS. The Lagrangian for the shell can be written as[14]

$$L = V_p - T_p \tag{1}$$

where V_p is the total potential energy associated with the strain energy of the DCS and the deformations of the restraint springs and T_p denotes the total kinetic energy of the shell. Both can be explicitly expressed as[15]

$$\begin{aligned}V_p=&\frac{G}{2}\int_0^{\theta_b}\int_0^{\varphi_a}\left(\varepsilon_\varphi^2+\varepsilon_\theta^2+2\nu\varepsilon_\varphi\varepsilon_\theta+\frac{1-\nu}{2}\varepsilon_{\varphi\theta}^2\right)R\mathrm{d}\varphi\mathrm{d}\theta+\\&\frac{D}{2}\int_0^{\theta_b}\int_0^{\varphi_a}\left(\kappa_\varphi^2+\kappa_\theta^2+2\nu\kappa_\varphi\kappa_\theta+2(1-\nu)\tau_{\varphi\theta}^2\right)R\mathrm{d}\varphi\mathrm{d}\theta+\\&\frac{1}{2}\int_0^{\varphi_a}\left[k^u_{\theta 0}u^2+k^v_{\theta 0}v^2+k^w_{\theta 0}w^2+K^w_{\theta 0}(v-\partial w/\partial\theta)^2/R_b^2\right]\Big|_{\theta=0}\cdot\\&R\mathrm{d}\varphi+\frac{1}{2}\int_0^{\varphi_a}\left[k^u_{\theta b}u^2+k^v_{\theta b}v^2+k^w_{\theta b}w^2+\right.\\&\left.K^w_{\theta b}(v-\partial w/\partial\theta)^2/R_b^2\right]\Big|_{\theta=\theta_b}R\mathrm{d}\varphi+\frac{1}{2}\int_0^{\theta_b}\left[k^u_{\varphi 0}u^2+\right.\\&\left.k^v_{\varphi 0}v^2+k^w_{\varphi 0}w^2+K^w_{\varphi 0}(u-\partial w/\partial\varphi)^2/R_a^2\right]\Big|_{\varphi=0}R\mathrm{d}\theta+\\&\frac{1}{2}\int_0^{\theta_b}k^u_{\varphi a}u^2+k^v_{\varphi a}v^2+k^w_{\varphi a}w^2+K^w_{\varphi a}(u-\\&\partial w/\partial\varphi)^2/R_a^2\Big]\Big|_{\varphi=\varphi_a}R\mathrm{d}\theta\end{aligned} \tag{2}$$

$$T_p=\frac{\rho h\omega^2}{2}\int_0^{\theta_b}\int_0^{\varphi_a}(w^2+u^2+v^2)R\mathrm{d}\varphi\mathrm{d}\theta \tag{3}$$

where D is the bending rigidity, $D=E(t)h^3/12(1-\nu^2)$; and G the extensional rigidity, $G=E(t)h/(1-\nu^2)$. $E(t)$, ν, ρ and ω are the temperature dependent Young's modulus[16], the Poisson's ratio, the mass density and the natural frequency of the DCS, respectively. φ_a and θ_b represent the value of φ at $\varphi=a$ and θ at $\theta=b$, respectively.

According to the Flugge thin-shell theory, the strain on the middle surface of the doubly curved shell can be expressed as[17]

$$\varepsilon_\varphi^0=\frac{1}{R_a}\frac{\partial u}{\partial\varphi}+\frac{w}{R_a} \tag{4}$$

$$\varepsilon_\theta^0=\frac{1}{R_b}\frac{\partial v}{\partial\theta}+\frac{w}{R_b} \tag{5}$$

$$\varepsilon_{\varphi\theta}^0=\frac{\partial}{\partial\theta}\left(\frac{u}{R_a}\right)+\frac{\partial}{\partial\varphi}\left(\frac{v}{R_b}\right) \tag{6}$$

where ε_φ^0, ε_θ^0 and $\varepsilon_{\varphi\theta}^0$ represent the total strains along the φ and θ directions and the shear strain in the

plane of the shell. The curvature and torsion of the noncentral surface of the doubly curved shell κ_x, κ_θ and $\tau_{x\theta}$ can be expressed as

$$\kappa_\varphi = \frac{1}{R_a}\frac{\partial}{\partial\varphi}\left(\frac{u}{R_a} - \frac{1}{R_a}\frac{\partial w}{\partial\varphi}\right) \tag{7}$$

$$\kappa_\theta = \frac{1}{R_b}\frac{\partial}{\partial\theta}\left(\frac{v}{R_b} - \frac{1}{R_b}\frac{\partial w}{\partial\theta}\right) \tag{8}$$

$$\tau_{\varphi\theta} = \left(\frac{u}{R_a^2} - \frac{1}{R_a^2}\frac{\partial w}{\partial\varphi}\right) + \left(\frac{v}{R_b^2} - \frac{1}{R_b^2}\frac{\partial w}{\partial\theta}\right) \tag{9}$$

Considering the thermal effect caused by temperature change, the thermal strain in the middle surface of the shell is[18]

$$\varepsilon_\varphi^T = \alpha_\varphi \Delta T, \varepsilon_\theta^T = \alpha_\theta \Delta T, \varepsilon_{\varphi\theta}^T = \alpha_{\varphi\theta}\Delta T \tag{10}$$

where α_φ, α_θ, $\alpha_{\varphi\theta}$ are the thermal expansion coefficients in φ, θ and tangential directions. ε_φ^T, ε_θ^T and $\varepsilon_{\varphi\theta}^T$ indicates the strains at temperature T and the superscript T represents the temperature. Then, the mechanical strains in the middle surface of the shell are

$$\varepsilon_\varphi = \varepsilon_\varphi^0 - \varepsilon_\varphi^T, \varepsilon_\theta = \varepsilon_\theta^0 - \varepsilon_\theta^T, \varepsilon_\beta = \varepsilon_{\varphi\theta}^0 - \varepsilon_{\varphi\theta}^T \tag{11}$$

The Spectro-Geometric method is adopted to construct the displacement functions[19]

$$\begin{aligned} w(\varphi,\theta) = &\sum_{m=0}^{\infty}\sum_{n=0}^{\infty} W_{mn}^1 \cos\lambda_m\varphi\cos\lambda_n\theta + \\ &\sum_{m=0}^{\infty}\sum_{n=1}^{4} W_{mn}^2 \cos\lambda_m\varphi\sin\lambda_n\theta + \\ &\sum_{m=1}^{4}\sum_{n=0}^{\infty} W_{mn}^3 \cos\lambda_n\theta\sin\lambda_m\varphi + \\ &\sum_{m=1}^{4}\sum_{n=1}^{4} W_{mn}^4 \sin\lambda_m\varphi\sin\lambda_n\theta \end{aligned} \tag{12}$$

$$\begin{aligned} u(\varphi,\theta) = &\sum_{m=0}^{\infty}\sum_{n=0}^{\infty} U_{mn}^1 \cos\lambda_m\varphi\cos\lambda_n\theta + \\ &\sum_{m=0}^{\infty}\sum_{n=1}^{2} U_{mn}^2 \cos\lambda_m\varphi\sin\lambda_n\theta + \\ &\sum_{m=1}^{2}\sum_{n=0}^{\infty} U_{mn}^3 \cos\lambda_n\theta\sin\lambda_m\varphi + \\ &\sum_{m=1}^{2}\sum_{n=1}^{2} U_{mn}^4 \sin\lambda_m\varphi\sin\lambda_n\theta \end{aligned} \tag{13}$$

$$\begin{aligned} v(\varphi,\theta) = &\sum_{m=0}^{\infty}\sum_{n=0}^{\infty} V_{mn}^1 \cos\lambda_m\varphi\cos\lambda_n\theta + \\ &\sum_{m=0}^{\infty}\sum_{n=1}^{2} V_{mn}^2 \cos\lambda_m\varphi\sin\lambda_n\theta + \\ &\sum_{m=1}^{2}\sum_{n=0}^{\infty} V_{mn}^3 \cos\lambda_n\theta\sin\lambda_m\varphi + \\ &\sum_{m=1}^{2}\sum_{n=1}^{2} V_{mn}^4 \sin\lambda_m\varphi\sin\lambda_n\theta \end{aligned} \tag{14}$$

where $\lambda_m = m\pi/\varphi_a$, $\lambda_n = n\pi/\theta_b$, $\boldsymbol{W}_{mn}$, $\boldsymbol{U}_{mn}$, and $\boldsymbol{V}_{mn}$ represent unknown coefficient vectors of displacement function series expansion of the shell; m and n are the wavenumbers in the φ-axis and θ-axis directions; and M and N are the numbers of truncation coefficients that are used.

Substituting Eqs. (12—14) of the DCS displacement into Eqs. (1—3) and minimizing the resulting equations against the unknown Fourier coefficients will lead to a set of couple systems

$$\{\boldsymbol{K} - \omega^2\boldsymbol{M}\}\{\boldsymbol{E}\} = \{\boldsymbol{0}\} \tag{15}$$

where $\boldsymbol{K}$ and $\boldsymbol{M}$ represent the stiffness matrix and mass matrix of the shell, respectively, and $\boldsymbol{E}$ represents the unknown coefficient vector of displacement function series expansion.

By solving Eq. (15), the natural frequency and the mode shapes of the doubly curved shell in thermal environment can be obtained.

2 Results and Discussion

With the theoretical model and formulations in the previous section, the natural frequencies and mode shapes of the doubly curved shell with a thermal environment under classical boundary conditions are analyzed in this section. The Young's modulus $E(t)$ of the material used in this paper varying with temperature is shown in Table 1. The thermal modal analysis of the doubly curved shell can be carried out according to the above material properties.

Table 1 Young's modulus of material at different temperatures

Temperature/ ℃	20	100	200	300	400
Young's modulus / GPa	203	206	182	153	141

2.1 Method validation

The formulations and the resulting model will be first validated against the results obtained by the finite element method (FEM). In Table 2, the first six natural frequencies for the DCS with completely free (FFFF) and clamped boundary (CCCC) conditions at 200 ℃ are examined. The material properties and geometrical dimensions used for the DCS

are given as follows: $\rho=2\ 700\ \mathrm{kg/m^3}$, $\nu=0.3$, $R_a=R_b=5$ m, $h=0.002$ m, $a=0.8$ m, $b=0.4$ m. The simply supported boundary condition (S) could be derived by setting the translational stiffness and the rotational stiffness to infinitely large and zero, respectively. The clamped boundary condition (C) is realized by setting the translational and rotational stiffnesses to infinitely large. For the free boundary condition (F), the translational and rotational stiffnesses are both set to zero.

Table 2 Comparison and convergence of the first six natural frequencies for DCS with completely free and clamped boundary conditions

Boundary condition	$M\times N$	Natural frequency / Hz					
		Mode 1	Mode 2	Mode 3	Mode 4	Mode 5	Mode 6
FFFF	8×8	30.987	32.993	73.668	84.625	129.74	141.06
	10×10	30.986	32.992	73.667	84.624	129.73	141.06
	12×12	30.986	32.992	73.666	84.623	129.73	141.06
	14×14	30.986	32.992	73.666	84.623	129.73	141.06
CCCC	FEM	30.935	32.904	73.455	84.463	129.34	140.83
	14×14	349.83	351.78	398.77	414.78	424.51	448.47
	FEM	349.89	351.82	398.75	414.55	424.09	448.17

It is clearly seen that the results agree well with each other. The convergence study of the truncated number of the improved Fourier series is also examined in Table 2. The results converge at $M=N=14$ for the given four-digital precision and numerical stability of the solution is evident. The above results completely prove the correctness of the method in this paper. To further validate the correctness of the

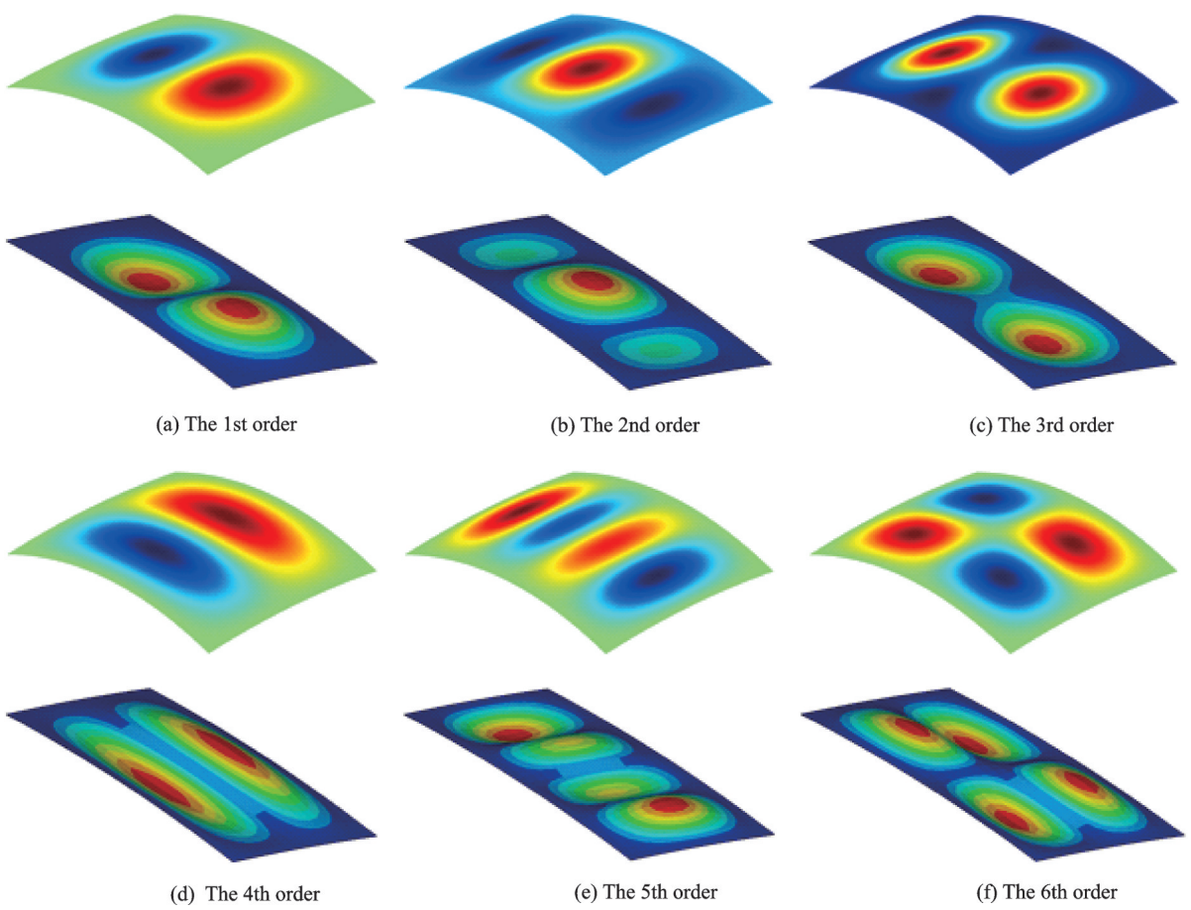

Fig.2 Comparisons of mode shapes of curved panel with completely clamped edges between present method and FEM (Upper plot: the present method; Lower plot: FEM)

present method, the first to sixth mode shapes of the curved panel under completely clamped edges (CCCC) are shown in Fig.2. Again, good agreement is observed between the two predictions.

2.2 Comparison of thermal modal frequency under classical boundary conditions

Fig.3 shows the first six natural frequencies for the DCS with a completely clamped boundary and a simply supported boundary at different temperatures. The material properties and geometrical dimensions used for the DCS are given as follows: ρ=2 700 kg/m^3, ν=0.3, R_a=R_b=4 m, h=0.002 m, a=0.5 m, b=0.3 m. Whether in Fig.3(a) or Fig.3(b), it is seen that when the modal number is determined, the modal frequency of the DCS will decrease with increasing temperature, but the temperature will not affect the change trend of the modal frequency.

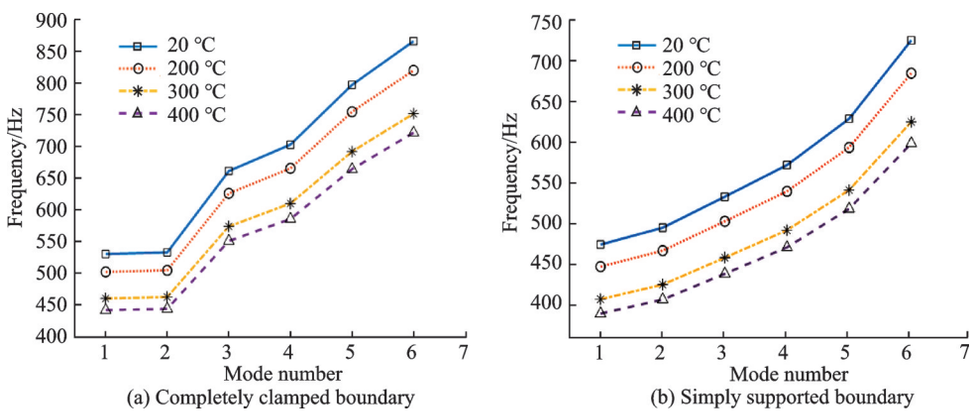

Fig.3 The first six natural frequencies for doubly curved shell at different temperatures

Fig.4 shows a comparison of the first eight natural frequencies for the doubly curved shell under different boundaries at 200 ℃. The material properties and geometrical dimensions used for the doubly curved shell are given as follows: ρ=2 700 kg/m^3, ν=0.3, R_a=R_b=3 m, h=0.002 m, a=0.4 m, b=0.4 m. The CSCS represents the clamped boundary at φ=0 and φ=a, and the simply supported boundary at θ=0 and θ=b. The SCSC represents the simply supported boundary at φ=0 and φ=a, and the clamped boundary at θ=0 and θ=b. It is clearly seen that the two curves of CSCS and SCSC coincide when the temperature is constant. This is because the DCS has symmetrical characteristics when a=b and R_a=R_b. The SSSS boundary condition has the lowest modal frequency and as the number of fixed edges increases, the modal frequency will also increase.

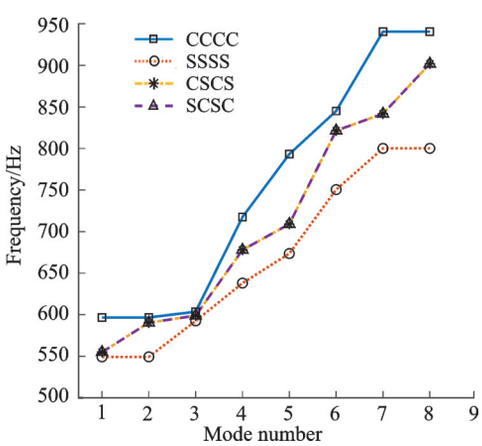

Fig.4 Comparison of the first eight natural frequencies for DCS under different boundaries at 200 ℃

The mode shapes of the DCS with different boundaries at 200 ℃ are plotted in Table 3, in which the first, third, fifth, eighth order of the mode shapes are randomly selected. The material properties are the same as in Fig.4. Since the frequencies of the doubly curved shell under CSCS boundary condition is the same as that under SCSC boundary condition, only the mode shapes of CSCS are analyzed. It is clearly seen that the mode shapes under different boundary conditions have small change but perceptible. With the increase of the numbers of fixed edges, the area where the peripheral displacement of the doubly curved shell is zero gradually increases, and the maximum vibration mode points gradually approach the center of the shell.

Table 3 Mode shapes of DCS with different boundaries at 200 ℃

Boundary condition	Mode number			
	1	3	5	8
SSSS	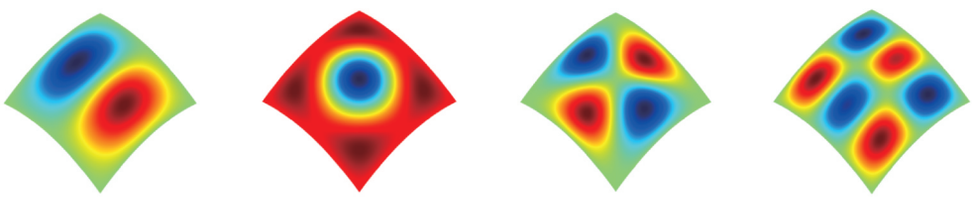			
CSCS	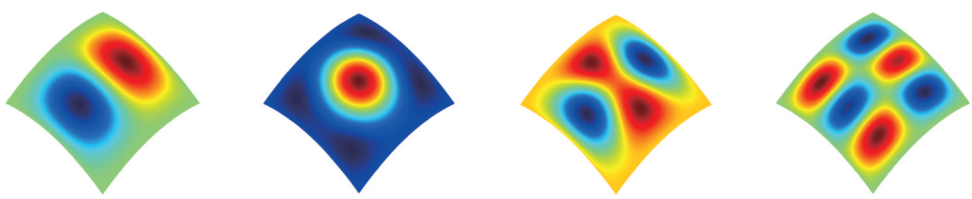			
CCCC	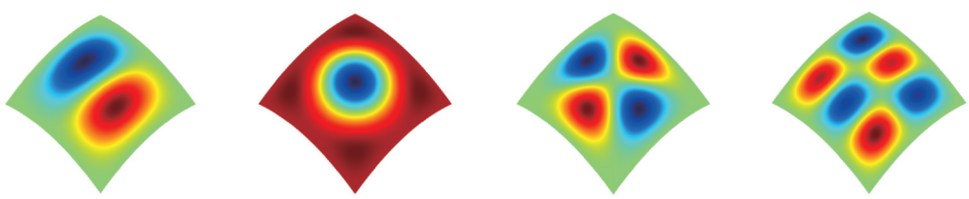			

2.3 Effects of structural parameters

Fig.5 shows the first natural frequencies for the doubly curved shell with different thicknesses under different temperatures. The material properties and geometrical dimensions used for the doubly curved shell are given as follows: $\rho=2\ 700\ \mathrm{kg/m^3}$, $\nu=0.3$, $R_a=R_b=4$ m, $a=0.2$ m, $b=0.2$ m. The boundary condition is a completely simply supported boundary. When h is constant, the modal frequency decreases with increasing temperature, which is the same as that in Fig.3. When the temperature is constant, the modal frequency increases with increasing h.

Fig.6 shows the first natural frequencies for the doubly curved shell with different curvature radii under different temperatures. The material properties and geometrical dimensions used for the doubly curved shell are given as follows: $\rho=2\ 700\ \mathrm{kg/m^3}$, $\nu=0.3$, $h=0.002$ m, $a=0.2$ m, $b=0.2$ m. The boundary condition is a completely simply supported

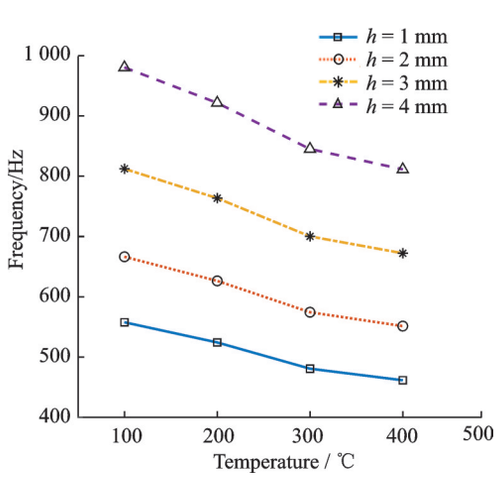

Fig.5 Comparison of the first natural frequencies for DCS with different thickness

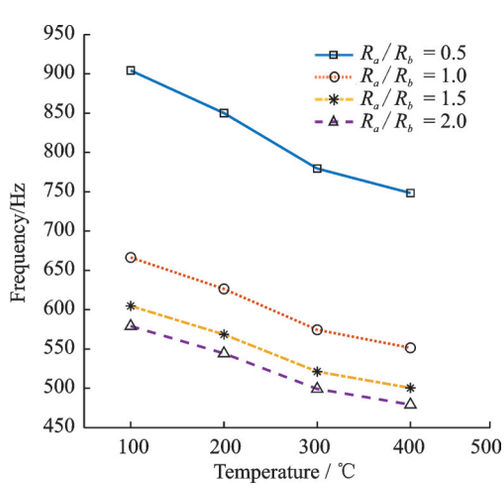

Fig.6 Comparison of the first natural frequencies for DCS with different curvature radius

boundary. When the temperature is constant, the modal frequency decreases with the increase of the ratio of R_a/R_b. When the ratio of R_a/R_b is constant, the modal frequency decreases with the increasing temperature, which is also consistent with that in Fig.3.

Fig.7 shows the first natural frequencies for the doubly curved shell with different ratios of a/b under different temperatures. The material properties and geometrical dimensions used for the doubly curved shell are given as follows: $\rho=2\ 700\ \mathrm{kg/m^3}$, $\nu=0.3$, $R_a=R_b=4$ m and $h=0.002$ m. The boundary condition is a completely simply supported boundary. It is clearly seen that the modal frequency decreases with the increase ratio of a/b at the same temperature. This is because the first natural frequency of the shell decreases with increasing DCS size.

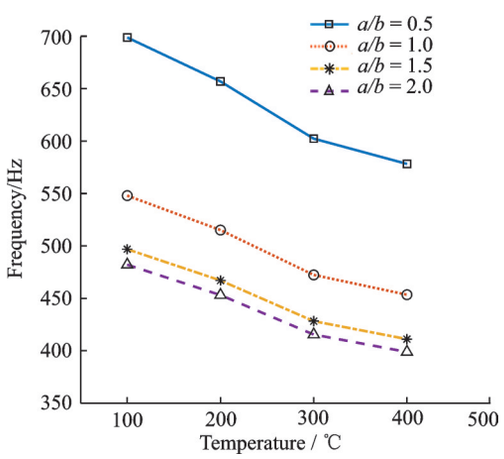

Fig.7 Comparison of the first natural frequencies for DCS with different ratio of a/b

3 Conclusions

In this paper, a theoretical model of the doubly curved shell under a steady thermal environment is established, and the natural frequency and mode shape of the doubly curved shell are solved by the Rayleigh-Ritz method. By setting several classical boundaries and different structural parameters, the modal frequencies of the doubly curved shell at several temperatures are analyzed. This paper mainly draws the following conclusions:

(1) The detailed solution process of the natural frequency and mode shape of the doubly curved shell in a thermal environment is established. It is verified that the results are stable when the truncation coefficient $M=N=14$, and the results show a good agreement with the finite element method under completely clamped and simply supported boundary conditions.

(2) Under the completely clamped and simply supported boundary conditions, the modal frequency decreases with increasing temperature. With increasing shell thickness, the first modal frequency decreases, which is opposite to that when R_a/R_b and a/b increase.

References

[1] HUU T H, THANH D H, MINH T T. Free vibration analysis of functionally graded doubly curved shell shells resting on elastic foundation in thermal environment[J]. International Journal of Advanced Structural Engineering, 2018, 10(3): 275-283.

[2] ALIJANI F, AMABILI M, KARAGIOZIS K, et al. Nonlinear vibrations of functionally graded doubly curved shallow shells[J]. Journal of Sound and Vibration, 2011, 330(7): 1432-1454.

[3] ALIJANI F, AMABILI M, BAKHTIARI N F. Thermal effects on nonlinear vibrations of functionally graded doubly curved shells using higher order shear deformation theory[J]. Composite Structures, 2011, 93(10): 2541-2553.

[4] YAZDI A A. Nonlinear vibration of thick multi-scale composite doubly curved shells[J/OL]. Mechanics Based Design of Structures and Machines, onlinepublished, 2020. DOI: 101080/15397734.2020.1760882.

[5] VIOLA E, TORNABENE F, FANTUZZI N. General higher-order shear deformation theories for the free vibration analysis of completely doubly-curved laminated shells and shells[J]. Composite Structures, 2013, 95: 639-666.

[6] SOFIYEV A H, TURAN F, ZERIN Z. Large-amplitude vibration of functionally graded orthotropic double-curved shallow spherical and hyperbolic paraboloidal shells[J]. International Journal of Pressure Vessels and Piping, 2020, 188: 104235.

[7] GHORBANPOUR A. Critical temperature of short cylindrical shells based on improved stability equation[J]. Journal of Applied Sciences, 2002. DOI: 10.3923/jas.2002.448.452.

[8] LI Y B, MO J, CHEN H Y. Thermal buckling and modal analysis of composite thin-cylindrical shells based on Rayleigh-Ritz method[J]. Science Technology and Engineering, 2019, 19(1): 250-255.

[9] TORNABENE F, FANTUZZI N, BACCIOCCHI M. A new doubly-curved shell element for the free vibrations of arbitrarily shaped laminated structures based on weak formulation isogeometric analysis[J]. Composite Structures, 2017, 171: 429-461.
[10] DASTJERDI S, AKGOZ B, CIVALEK O, et al. On the non-linear dynamics of torus-shaped and cylindrical shell structures[J]. International Journal of Engineering Science, 2020, 156: 103371.
[11] DASTJERDI S, MALIKAN M, EREMEYEV V A, et al. Mechanical simulation of artificial gravity in torus-shaped and cylindrical spacecraft[J]. ACTA Astronautica, 2021, 179: 330-344.
[12] DASTJERDI S, MALIKAN M, EREMEYEV V A, et al. On the generalized model of shell structures with functional cross-sections[J]. Composite Structures, 2021, 272: 114192.
[13] KARIMIASL M, EBRAHIMI F, AKGOZ B. Buckling and post-buckling responses of smart doubly curved composite shallow shells embedded in SMA fiber under hygro-thermal loading[J]. Composite Structures, 2019, 223: 110988.
[14] LEISSA A W, LEE J K, WANG A J. Vibrations of cantilevered doubly curved shallow shells[J]. International Journal of Solids and Structures, 1983, 19(5): 411-424.
[15] YE T G, JIN G Y, CHEN Y H, et al. A unihed formulation for vibration analysis of open shells with arbitrary boundary conditions[J]. International Journal of Mechanical Sciences, 2014, 81: 42-59.
[16] HAMAZAH A A, JOBAIR H K. An investigation of dynamic behavior of the cylindrical shells under thermal effect[J]. Case Studies in Thermal Engineering, 2018, 12: 537-545.
[17] LEISSA A W, NARITA Y. Vibrations of completely free shallow shells of rectangular planform[J]. Journal of Sound and Vibration, 1984, 96(2): 207-218.
[18] AREFI M. An analytical investigation on free vibration of FGM doubly curved shallow shells with stiffeners under thermal environment[J]. European Journal of Mechanics A-Solids, 2015, 40: 181-190.
[19] WANG G, LI W L, DU J T, et al. Prediction of break-out sound from a rectangular cavity via an elastically mounted panel[J]. Journal of the Acoustical Society of America, 2016, 139(2): 684-692.

Acknowledgements This work was supported by the National Natural Science Foundation of China(No. 51805341) and the Natural Science Foundation of Jiangsu Province (No. BK20180843).

Authors Mr. **ZHANG Yongfeng** received the B.S. degree from School of Mechanical and Electrical Engineering, Soochow University in 2020, and is currently pursuing MA. Eng in the School of Mechanical and Electrical Engineering, Soochow University.

Prof. **WANG Gang** received the B.E. and Ph.D. degrees from Harbin Engineering University, Harbin, China, in 2010 and 2016, respectively. From 2013 to 2015, he was pursuing a co-training Ph.D. at Wayne State University. His research interests include dynamics analysis, vibration and noise control, etc. At present, he has presided over one national Natural Science Foundation Project, three provincial and ministerial projects.

Author contributions Mr. **ZHANG Yongfeng** completed the calculation of data results and simulation comparison, and wrote the third and fourth parts of the manuscript. Mr. **ZHU Ziyuan** integrated the theoretical model and completed the first and second parts of the manuscript. Prof. **WANG Gang** designed the study, complied the models, and reviewed the manuscript. All authors commented on the manuscript draft and approved the submission.

Competing interests The authors declare no competing interests.

(Production Editor: SUN Jing)

基于瑞利-里兹法的双曲面壳热模态分析

张永锋，朱梓渊，王　刚

(苏州大学机电工程学院，苏州 215131，中国)

摘要：双曲面壳(Doubly curved shell, DCS)是工程领域中常见的结构形式。在热环境中，DCS的振动特性将受到热效应的影响，但对DCS在热环境中振动特性的研究相对有限。本文研究了由温度变化引起的热应变和杨氏模量的变化，系统地建立了DCS能量方程。使用谱几何方法构造了DCS的位移容限函数，使用瑞利-里兹法求解了不同结构参数(如厚度、R_a/R_b和a/b比)的DCS在不同温度下的固有频率和振型。结果表明，DCS的固有频率随温度、R_a/R_b和a/b比的增加而降低，随厚度的增加而增加。

关键词：双曲面壳体；热环境；瑞利-里兹法；固有频率